

# Reports

## Serpentine Minerals: Intergrowths and New Combination Structures

**Abstract.** *The serpentine minerals chrysotile, lizardite, and antigorite have been found intimately intergrown with each other and with talc, chlorite, and amphibole in incompletely reacted chain silicates. High-resolution transmission electron microscopy has revealed new variations in serpentine planar and roll structures, as well as regions of mixed-layer silicate consisting of serpentine and talc layers.*

The serpentine minerals are of both economic and petrologic interest. Roughly 95 percent of the asbestos used worldwide is the chrysotile variety of serpentine, and serpentinite bodies play an important role in the events that occur during mountain building. Serpentine minerals typically form either by a hydration reaction of olivine and chain silicates or by reaction of dolomite with silica-rich fluids. Likewise, micas and talc are also common alteration products of pyroxenes and amphiboles. Recent x-ray and high-resolution transmission electron microscopy (HRTEM) studies have shown that the mechanisms of these alteration reactions are complex and variable (1). The present study demonstrates that this complexity extends to hydration reactions involving serpentine minerals, as suggested earlier by textural and x-ray investigations (2).

In this report, we describe HRTEM observations on two mineral occur-

rences in which pyroxene and amphibole have reacted to form intergrowths of structurally disordered amphibole, talc, and the serpentine minerals chrysotile, lizardite, and antigorite. These intergrowths reveal new variations in serpentine crystal structure, demonstrate that serpentine and talc layers can intergrow intimately, and underline the observation that solid-state silicate reactions can result in highly complex, disequilibrium mineral mixtures.

The specimens that we used in this study are an anthophyllite (orthoamphibole) from the Cascade Mountains, Washington (3), and a uralite (pyroxene reacted to "amphibole") from Ocna de Fier, Romania (4). Thin specimens were prepared normal to the chain silicate *c*-axis by argon ion bombardment, and they were observed with HRTEM techniques described in (5). Image interpretation was based on observations and dynamical imaging calculations showing

that, under appropriate conditions, chain width can be deduced from *c*-axis images of chain silicates, and micas, talc, chlorites, and serpentines produce (00 $\ell$ ) fringes that in some cases are embellished with spots related to interlayer site positions (5, 6). Serpentine minerals can be distinguished from most other sheet silicates by the smaller (00 $\ell$ ) fringe spacing (Table 1).

Serpentine minerals consist of stacks of layers that contain a silicate sheet bonded to a sheet of octahedrally coordinated magnesium ions. Micas and talc, on the other hand, consist of layers having silicate sheets on both sides of the octahedral sheet (7). Whereas mica and talc layers are usually planar, serpentine layers can have a variety of configurations (Table 1). Yada has produced pioneering HRTEM images of chrysotile asbestos viewed parallel to the fibers; these images directly reveal the rolled and cylindrical structures (8).

Investigation by HRTEM has shown that part of the Cascades anthophyllite specimen consists of amphibole, talc, chrysotile, and lizardite in contact or within a few tens of angstroms of each other (Fig. 1). Most of the specimen is anthophyllite with numerous triple, quadruple, and wider chains, intergrown with talc. Serpentine is rare, but, where it does occur, it is near the chain silicate.

Serpentine is much more abundant in the Romanian uralite specimen than in the anthophyllite, although it is again most abundant in regions near amphibole. In addition to lizardite and well-formed rolls of chrysotile, there are antigorite and a number of hitherto unobserved serpentine configurations. Figure 2a shows amphibole, talc, and planar serpentine intergrown with partial serpentine rolls. These festoons can be thought of as incomplete chrysotile fibers connected by lizardite. Another type of planar-roll combination is shown in Fig. 2b, where lizardite sheets terminate in more complete rolls. One of these rolls shows a reversal in the direction of curvature, and some of the sheets double back on themselves, producing a hairpin configuration. Other newly observed variations in serpentine structure include undulation structures having wavelengths of about 150 Å, "braiding" of curved and planar serpentine, and splaying of the sheets in partial rolls. It is common to observe crossing of the (00 $\ell$ ) fringes in these new structures; this result suggests that they are not very extensive in the direction of the axes of curvature. On the other hand, crossing of fringes in the complete chrysotile rolls

Table 1. Mineral structures, compositions, and (00 $\ell$ ) fringe spacings; "M" refers to octahedral cations, such as Mg, Fe, Ca, or Mn.

Mineral	Structure	Composition	(00 $\ell$ ) fringe spacing (Å)
Serpentines			
Chrysotile	Cylindrical or rolled sheet silicate	Mg <sub>3</sub> Si <sub>2</sub> O <sub>5</sub> (OH) <sub>4</sub>	7.3
Lizardite	Planar sheet silicate	Mg <sub>3</sub> Si <sub>2</sub> O <sub>5</sub> (OH) <sub>4</sub>	7.3
Antigorite	Corrugated sheet silicate	Mg <sub>3-x</sub> Si <sub>2</sub> O <sub>5</sub> (OH) <sub>4-2x</sub>	7.3
Biopyriboles			
Pyroxene	Single-chain silicate	MSiO <sub>2</sub>	
Amphibole	Double-chain silicate	M <sub>7</sub> Si <sub>8</sub> O <sub>22</sub> (OH) <sub>2</sub>	
Talc	Planar sheet silicate	Mg <sub>3</sub> Si <sub>4</sub> O <sub>10</sub> (OH) <sub>4</sub>	9.3
Trioctahedral mica	Planar sheet silicate	(K,Na)M <sub>3</sub> Si <sub>3</sub> AlO <sub>10</sub> (OH) <sub>4</sub>	10
Chlorite	Planar sheet silicate	(M,Al) <sub>2</sub> (Si,Al) <sub>4</sub> O <sub>10</sub> (OH) <sub>2</sub>	14
Brucite	Planar sheet hydroxide	Mg(OH) <sub>2</sub>	4.8

has not been observed; this is consistent with long fibers.

In parts of the uralite specimen, serpentine and talc form fine intergrowths that can be recognized either by electron diffraction or by high-resolution imaging. Mixed-layer intergrowths of this kind can be described as belonging to a polysomatic series (9) between the serpentine and talc structures. Similarly, fine intergrowths of serpentine and brucite layers have recently been observed in carbonaceous chondrite matrices (10), demonstrating analogous polysomaticism between these structures. In a few parts of the uralite, there is also chlorite structure, which consists of alternating talc-like and brucite layers. The images of this material are similar to those produced by well-characterized chlorites (11); this 14-Å structure forms intimate intergrowths with serpentine and talc.

These serpentine-talc-chlorite-amphibole intergrowths demonstrate that retrograde hydration reactions of chain silicates can result in complex dis-

equilibrium mineral mixtures. Textural relationships suggest that in the uralite specimen pyroxene was first converted to amphibole, which in turn became structurally disordered by the growth of wide-chain material and talc. Similarly, the anthophyllite specimen was partially converted to wide-chain silicate and talc. After this stage, the serpentine-talc intergrowths apparently grew: this interpretation is consistent with the textural relationships of Fig. 2a, for example, in which the serpentine-talc region cuts across chain-width errors in the amphibole. The notion that the serpentine minerals grew from amphibole in the late stages of alteration is also supported by their proximity to or contact with the amphibole. Serpentine is not found in the talc far from chain silicate, and this talc presumably formed from the amphibole in the earlier stages of hydration.

Stability studies (12) suggest that, in addition to temperature and pressure controls, serpentine minerals form in environments with lower  $H_4SiO_4$  activity or

higher magnesium activity than required for talc and anthophyllite. In particular, the experiments by Hemley *et al.* (12) demonstrate that, at constant pressure, the silica concentration in equilibrium with talc plus serpentine must be lower than that in equilibrium with anthophyllite. If the activity coefficient of  $H_4SiO_4$  is assumed to be unity (appropriate for uncharged species in dilute solution), then the change in alteration sequence from amphibole  $\rightarrow$  talc to amphibole  $\rightarrow$  talc + serpentine could be explained by a drop in the activity of  $H_4SiO_4$  during the final stages of the retrograde hydration reaction. The textural relations further show that chrysotile, antigorite, and lizardite can all grow in intimate contact during the solid-state alteration of chain silicates.

These serpentine-bearing intergrowths may also be important from the standpoint of occupational health. Large doses of asbestos dust have been implicated as causes of asbestosis and lung cancer (13), although there is some evi-

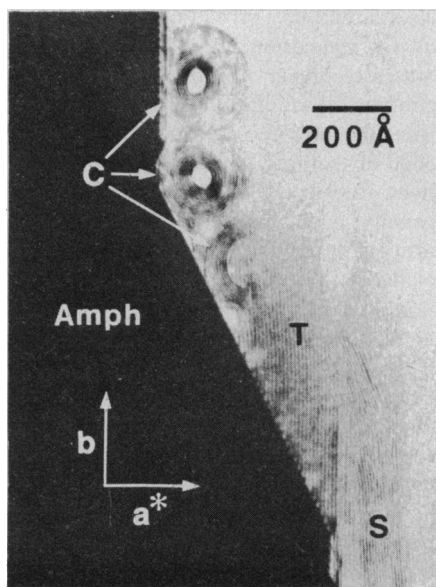
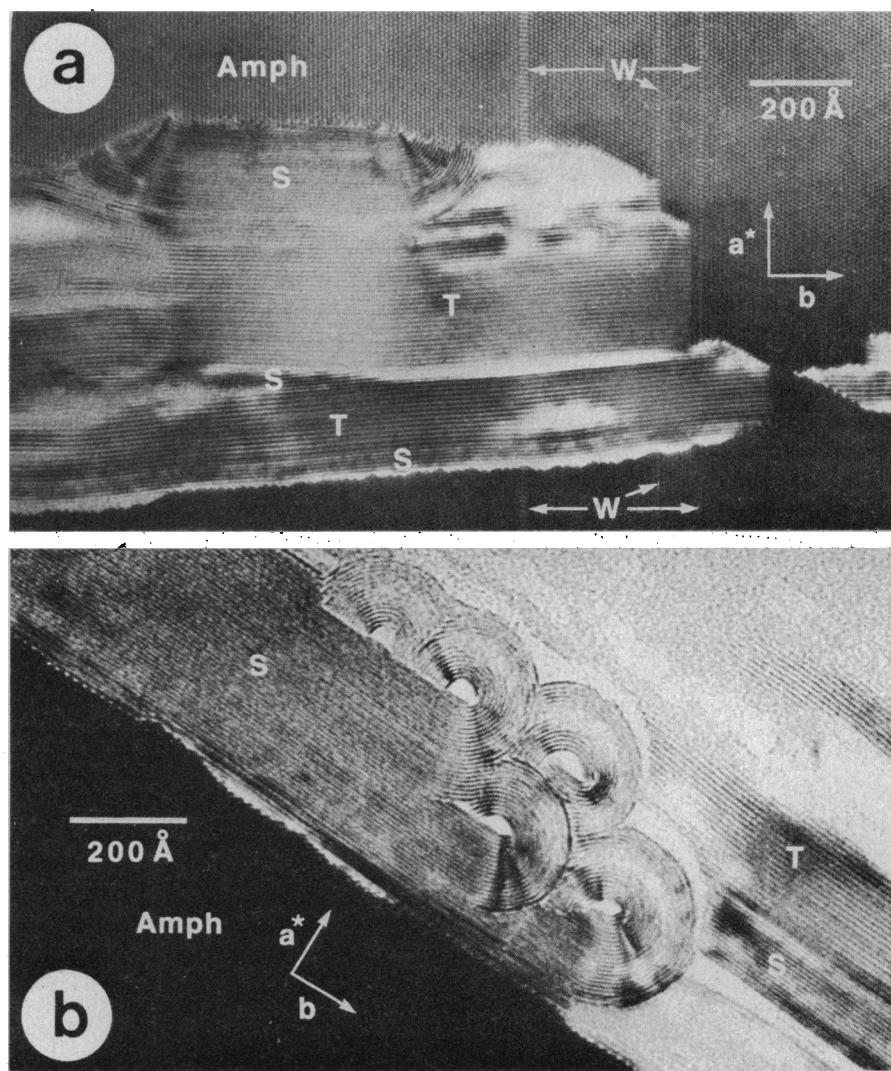


Fig. 1 (above). An HRTEM photograph of planar serpentine (S), chrysotile (C), talc (T), and amphibole (Amph) in the Cascades anthophyllite specimen. Talc and serpentine are differentiated by fringe spacing (Table 1), and chrysotile shows its characteristic curved layers (8). The crystallographic axes refer to amphibole. Fig. 2 (right). The HRTEM photographs of combination planar and roll serpentine structures in Romanian uralite specimen. (a) Partial roll forms abutting against chain silicate (Amph). Areas of talc (T) and serpentine (S) can be recognized by the fringe spacing (Table 1). Chain-width errors (W) in the amphibole are cut by the region of serpentine and talc. The crystallographic axes refer to amphibole. (b) Planar serpentine (lizardite) ending in rolls. In one of the rolls, the direction of curvature reverses, producing a hair-pin structure.



dence that chrysotile may be relatively harmless as compared to some types of amphibole asbestos (14). The sub-microscopic chrysotile that occurs within altered chain silicates probably does not pose a major health hazard to the general population. However, possible detrimental effects for miners working in the vicinity of deposits containing abundant altered pyroxene should not be overlooked. In particular, it is possible that significant amounts of chrysotile dust could be generated during mining operations in skarn deposits, such as the one from which the uraltite specimen was taken. In view of the intimate geometry of the intergrowths, individual chrysotile fibers may not even be liberated during mining, but dusts produced during such operations should, at least, be monitored for chrysotile content.

DAVID R. VEBLER  
PETER R. BUSECK

Departments of Geology and  
Chemistry, Arizona State  
University, Tempe 85281

#### References and Notes

1. D. R. Veblen, P. R. Buseck, C. W. Burnham, *Science* **198**, 359 (1977); D. R. Veblen and C. W. Burnham, *Am. Mineral.* **63**, 1000 (1978); *ibid.*, p. 1053.
2. F. J. Wicks and E. J. W. Whittaker, *Can. Mineral.* **15**, 459 (1977); J. Zussman, *ibid.*, p. 446.
3. Collected by Dr. P. Misch at the locality described on page 42 in *Geological Excursions in the Pacific Northwest*, E. Brown and R. Ellis, Eds. (Geological Society of America, Boulder, Colo., 1977). The structural formula of the anthophyllite is  $Mg_2Fe_2Ca_2Si_8O_{22}(OH)_2$ .
4. Collected by Dr. D. M. Burt at Juliana Quarry, Ocna de Fier, Romania. The amphibole is primitive and contains Mg, Fe, and Mn. It was too finely intergrown with calcite and other phases to permit quantitative analysis.
5. D. R. Veblen and P. R. Buseck, *Am. Mineral.* **64**, 687 (1979); in preparation.
6. S. Iijima and P. R. Buseck, *Acta Crystallogr. Sect. A* **34**, 709 (1978); K. Yada and K. Iishi, *Am. Mineral.* **62**, 958 (1977).
7. F. J. Wicks and E. J. W. Whittaker, *Can. Mineral.* **13**, 227 (1975); W. A. Deer, R. A. Howie, J. Zussman, *Rock-Forming Minerals* (Wiley, New York, 1962), vol. 3.
8. K. Yada, *Acta Crystallogr.* **23**, 704 (1967); *Acta Crystallogr. Sect. A* **27**, 659 (1971).
9. J. B. Thompson, *Am. Mineral.* **63**, 239 (1978).
10. I. D. R. Mackinnon and P. R. Buseck, *Nature (London)* **280**, 219 (1979); T. R. McKee and C. B. Moore, *Lunar Planet. Sci.* **10**, 807 (1979).
11. S. Iijima and P. R. Buseck, *Eos* **58**, 524 (1977).
12. J. J. Hemley, J. W. Montoya, C. L. Christ, P. B. Hostetter, *Am. J. Sci.* **277**, 322 (1977); J. J. Hemley, J. W. Montoya, D. R. Shaw, R. W. Luce, *ibid.*, p. 353; B. W. Evans, W. Johannes, H. Oterdoom, V. Trommsdorff, *Schweiz. Mineral. Petrogr. Mitt.* **56**, 79 (1976).
13. I. J. Selikoff, J. Churg, E. C. Hammond, *J. Am. Med. Assoc.* **188**, 22 (1964); R. L. Zielhuis, *Public Health Risks of Exposure to Asbestos* (Pergamon, Oxford, 1977).
14. M. Ross, in *Workshop on Asbestos: Definitions and Measurement Methods*, C. C. Gravatt, Ed. (Special Publication 503, National Bureau of Standards, Gaithersburg, Md., 1978), p. 49.
15. Specimens were kindly supplied by P. Misch, K. Krupka, and D. M. Burt. We thank I. D. R. Mackinnon and T. R. McKee for helpful discussions and J. Clark for microprobe analysis. The electron microscopy was performed in the Center for Solid State Science, Arizona State University, and was supported by NSF grants EAR77-00128 and AENV76-17130.

19 March 1979; revised 7 May 1979

## Phanerozoic Land-Plant Diversity in North America

**Abstract.** A strong correlation exists between the outcrop area of nonmarine rocks deposited during a given geologic period and the observed vascular plant diversity for the same period; however, diversity residuals characteristic of certain periods may have underlying biological causes. Within-flora diversity changes through time indicate that stepwise increases in community species packing have accompanied major tracheophyte evolutionary innovations. Total and within-flora data suggest that the track of North American land-plant diversity has been similar in nature, but not in timing, to that inferred for marine invertebrates.

Changes in diversity can provide substantial insight into the tempo and mode of evolution of vascular land plants (1) and, in addition, can furnish an "out-group" comparison for models of biotic diversity change based on the fossil record of marine invertebrates (2-4). We now present a preliminary survey of vascular plant diversity, drawn from a compilation of more than 7500 Silurian to Tertiary plant species, predominantly from North America.

Many of the arguments proposed for the interpretation of the marine invertebrate record apply to the analysis of vascular plant diversity; it is important, however, to recognize that land plants are subject to unique biases (5). (i) Vascular plants show indeterminate growth and significant intraspecific or even intraorganismal morphologic variation. (ii) Vascular plants are rarely preserved in toto; thus organ and form genera cause over- and underestimates of diversity, respectively. (iii) Most land plants inhabit areas of net sediment erosion rather than areas of net sediment accumulation.

If these paleobotanical limitations are borne in mind, the plant fossil record provides an independent and reliable data bank of taxa for interpreting evolutionary phenomena. Figure 1A illustrates the time-standardized diversity of 7500 species plotted by geologic age. The data suggest that species diversity of land plants in North America rose to a relative maximum in the Carboniferous, dropped during the later Permian, and, after a Mesozoic period of low values, rose sharply during the Cretaceous and Tertiary. Figure 1B shows the time-standardized outcrop area of nonmarine sedimentary rocks in each geologic period for the United States and Canada. (The contribution of Mexican and Central American fossil species is negligible.) The linear regression of diversity versus outcrop area can be described by the equation: number of species per million years =  $0.0034 \text{ km}^2$  per million years + 15.5. In this case,  $r = .868$ ; if only the period from the Permian to the Jurassic is considered,  $r = .995$ . Thus,

Raup's (2) admonition that the availability of unmetamorphosed sedimentary rock influences the number of reported fossil taxa is applicable to the paleobotanical record. The correlation for plant data is by no means perfect. Residual diversity values exist for the Devonian, Cretaceous-Tertiary, and, to a lesser extent, the Carboniferous. These periods are associated with major evolutionary innovations in the plant kingdom—the origin and initial radiation of vascular land plants (Devonian), the evolution of heterospory and the seed (Devonian-Carboniferous), and angiospermy (Cretaceous-Tertiary). Various geologic factors may also have contributed to residuals indirectly by providing physical stimuli for speciation and via time-variable biases of preservation: (i) differences in continental sedimentary rocks characteristic for each geologic period, (ii) influence of tectonic modes on species turnover rates, (iii) environmental heterogeneity and climate alteration due to orogenesis, and (iv) variations in provinciality.

Carbonaceous sedimentary rocks are not equally represented in all periods (6); Carboniferous, Cretaceous, and Tertiary continental rocks contain relatively large amounts of coal per unit of outcrop area: 1.13, 0.56, and 0.69 million short tons of coal per square kilometer of outcrop. Sediment quality is not the sole factor in explaining diversity residuals, however; the Devonian residual is not associated with an abundance of organic-rich sediments. The floral biostratigraphic zonation of Pennsylvanian cyclothem illustrates the apparent correlation of turnover rates with tectonic events (7). Similarly, environmental heterogeneity resulting from tectonic uplift may influence Tertiary diversity data. The Laramide orogeny and the climatic deterioration beginning in the early Oligocene (8) may have increased diversity by increasing the number of available niches. Additionally, the superimposition of western North American Tertiary volcanism on this environmental pattern may have increased the number of habitats from which plants were preserved. Volcanic-